Article

Using Spin Dynamics of Covalently Linked Radical Ion Pairs To Probe the Impact of Structural and Energetic Changes on Charge Recombination

Shulamit Shaakov, Tamar Galili, Eli Stavitski, Haim Levanon, Aaron Lukas, and Michael R. Wasielewski

J. Am. Chem. Soc., **2003**, 125 (21), 6563-6572• DOI: 10.1021/ja034356x • Publication Date (Web): 02 May 2003

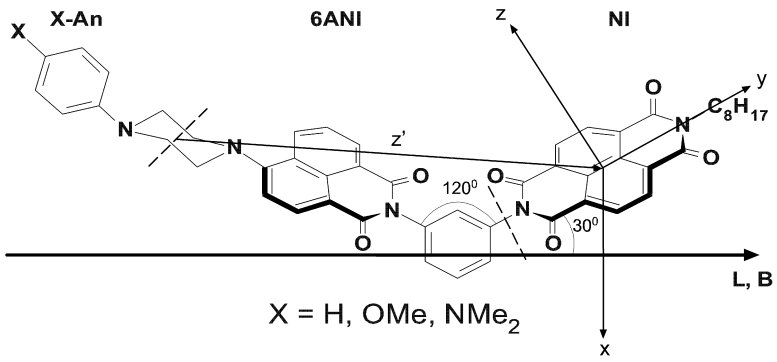

More About This Article

Additional resources and features associated with this article are available within the HTML version:

- Supporting Information
- Links to the 3 articles that cite this article, as of the time of this article download
- Access to high resolution figures
- Links to articles and content related to this article
- Copyright permission to reproduce figures and/or text from this article

View the Full Text HTML

J|A|C|S
ARTICLES
Published on Web 05/02/2003

Using Spin Dynamics of Covalently Linked Radical Ion Pairs To Probe the Impact of Structural and Energetic Changes on Charge Recombination

Shulamit Shaakov,[†] Tamar Galili,[†] Eli Stavitski,[†] Haim Levanon,*[,†] Aaron Lukas,[‡] and Michael R. Wasielewski*[,‡]

Contribution from the Department of Physical Chemistry and the Farkas Center for Light-Induced Processes, The Hebrew University of Jerusalem, Jerusalem 91904, Israel, and Department of Chemistry and Center for Nanofabrication and Molecular Self-Assembly, Northwestern University, Evanston, Illinois 60208-3113

Received January 27, 2003; E-mail: wasielew@chem.northwestern.edu; levanon@chem.ch.huji.ac.il

Abstract: We have synthesized a series of structurally related, covalently linked electron donor−acceptor triads having highly restricted conformations to study the effects of radical ion pair (RP) structure, energetics, and solvation on charge recombination. The chromophoric electron acceptor in these triads is a 4-aminonaphthalene-1,8-dicarboximide (6ANI), in which the 4-amine nitrogen atom is part of a piperazine ring. The second nitrogen atom of the piperazine ring is part of a para-substituted aniline donor, where the para substituents are X = H, OMe, and NMe_2. The imide group of 6ANI is linked to a naphthalene-1,8:4,5-bis(dicarboximide) (NI) electron acceptor across a phenyl spacer in a meta relationship. The triads undergo two-step photoinduced electron transfer to yield their respective $XAn^{\bullet+}$-6ANI-Ph-$NI^{\bullet-}$ RP states, which undergo radical pair intersystem crossing followed by charge recombination to yield ^{3}*NI. Time-resolved electron paramagnetic resonance experiments on the spin-polarized RPs and triplet states carried out in toluene and in E-7, a mixture of nematic liquid crystals (LCs), show that for all three triads, the $XAn^{\bullet+}$-6ANI-Ph-$NI^{\bullet-}$ RPs are correlated radical pairs and directly yield values of the spin−spin exchange interaction, *J*, and the dipolar interaction, *D*. The values of *J* are all about −1 mT and show that the LC environment most likely enforces the chair conformation at the piperazine ring, for which the RP distance is larger than that for the corresponding boat conformation. The values of *D* yield effective RP distances that agree well with those calculated earlier from the spin distributions of the radical ions. Within the LC, changing the temperature shows that the CR mechanism can be changed significantly as the energy levels of the RPs change relative to that of the recombination triplet.

Introduction

The bacterial photosynthetic reaction center is the classic example of an electron donor−acceptor system having highly restricted spatial relationships between the redox cofactors. Charge separation (CS) within this protein is initiated by electron transfer (ET) from the lowest excited state of a bacteriochlorophyll dimer (P) to an adjacent bacteriochlorophyll (B), followed by sequential thermal ET to bacteriopheophytin (H), and finally to a quinone (Q), forming the $P^{\bullet+}$-B-H-$Q^{\bullet-}$ radical ion pair (RP) in about 200 ps.[1−5] Removal or chemical reduction of Q, followed by photoexcitation produces the $P^{\bullet+}$-B-$H^{\bullet-}$ RP, which is formed in a pure singlet state. The $^1[P^{\bullet+}$-B-$H^{\bullet-}]$ singlet state undergoes S−T mixing with the three sublevels of the RP triplet state, $^1[P^{\bullet+}$-B-$H^{\bullet-}] \leftrightarrow {}^3[P^{\bullet+}$-B-$H^{\bullet-}]$, driven primarily by the electron−nuclear hyperfine interactions within each radical ion of the pair. Subsequent RP recombination produces ^{3}*P-B-H via the radical pair intersystem crossing mechanism (RP-ISC). The spin dynamics that accompany the ET events within these proteins provide an important probe of both the electronic structure of the reaction center and the electronic coupling matrix elements, *V*, for the various ET processes.

Among the numerous donor−acceptor systems synthesized to mimic the ET dynamics of photosynthetic bacteria, spin-selective charge recombination (CR) to a localized triplet state of the donor or the acceptor has been observed in only a few cases.[6−11] Our previous work demonstrated the first donor−

[†] The Hebrew University of Jerusalem.
[‡] Northwestern University.

(1) Ogrodnik, A.; Michel-Beyerle, M. E. *Z. Naturforsch.* **1989**, *44a*, 763−764.
(2) DiMagno, T. J.; Norris, J. R. In *The Photosynthetic Reaction Center*; Deisenhofer, J., Norris, J. R., Eds.; Academic Press: San Diego, 1993; Vol. 2, pp 105−133.
(3) Sumi, H.; Kakitani, T. *Chem. Phys. Lett.* **1996**, *252*, 85−93.
(4) Plato, M.; Mobius, K.; Michel-Beyerle, M. E.; Bixon, M.; Jortner, J. *J. Am. Chem. Soc.* **1988**, *110*, 7279−7285.
(5) Holzapfel, W.; Finkele, U.; Kaiser, W.; Oesterhelt, D.; Scheer, H.; Stilz, H. U.; Zinth, W. *Chem. Phys. Lett.* **1989**, *160*, 1−7.
(6) Hasharoni, K.; Levanon, H. *J. Phys. Chem.* **1995**, *99*, 4875−4878.
(7) Hasharoni, K.; Levanon, H.; Greenfield, S. R.; Gosztola, D. J.; Svec, W. A.; Wasielewski, M. R. *J. Am. Chem. Soc.* **1996**, *118*, 10228−10235.
(8) Carbonera, D.; DiValentin, M.; Corvaja, C.; Agostini, G.; Giacometti, G.; Liddel, P. A.; Kuciauskas, D.; Moore, A. L.; Moore, T. A.; Gust, D. *J. Am. Chem. Soc.* **1998**, *120*, 4398−4405.
(9) Wiederrecht, G. P.; Svec, W. A.; Wasielewski, M. R.; Galili, T.; Levanon, H. *J. Am. Chem. Soc.* **1999**, *121*, 7726−7727.
(10) Wiederrecht, G. P.; Svec, W. A.; Wasielewski, M. R.; Galili, T.; Levanon, H. *J. Am. Chem. Soc.* **2000**, *122*, 9715−9722.

Chart 1

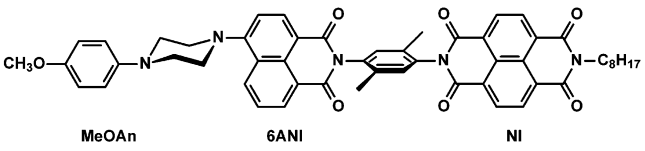

Chart 2

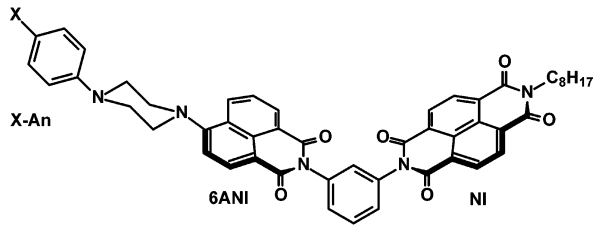

X = H, OMe, NMe_2

acceptor molecule, MeOAn-6ANI-Me_2Ph-NI (Chart 1), to closely mimic the spin-dependent CR dynamics within the photosynthetic reaction center.[6,7,12] Transient absorption spectroscopy in toluene determined that excitation of the 6ANI chromophore results in stepwise CS, MeOAn-^{1}*6ANI-Me_2Ph-NI → MeOAn$^{\bullet+}$-6ANI$^{\bullet-}$-Me_2Ph-NI → MeOAn$^{\bullet+}$-6ANI-Me_2-Ph-NI$^{\bullet-}$, to form the final RP with a quantum yield of 0.92. This RP undergoes S−T mixing to yield ^{3}[MeOAn$^{\bullet+}$-6ANI-Me_2Ph-NI$^{\bullet-}$], which recombines to give a high yield of MeOAn-6ANI-Me_2Ph-^{3}*NI via RP-ISC. The sublevels of this localized triplet state have unique non-Boltzmann spin populations, which result in spin-polarized electron paramagnetic resonance (EPR) spectra that closely mimic those observed for reaction centers, and can be detected using time-resolved EPR (TREPR) spectroscopy.[13−16] Subsequently, Gust and co-workers studied a donor−acceptor triad based on a chromophoric porphyrin donor coupled to a fullerene electron acceptor and a carotenoid secondary donor that also displays the TREPR spin polarization pattern characteristic of RP-ISC.[8,17] The spin dynamics of RP recombination on the picosecond scale have also been observed using applied magnetic fields of several teslas in ferrocene complexes.[18]

We have recently developed a variety of donor−acceptor structural motifs based on the components that comprise the molecule shown in Chart 1. We have synthesized a family of closely related triads having highly restricted conformations to study the effects of RP energies on their spin dynamics (Chart 2). The chromophoric electron acceptor in these triads is a 4-aminonaphthalene-1,8-dicarboximide (6ANI), in which the 4-amine nitrogen atom is part of a piperazine ring. The second nitrogen atom of the piperazine ring is part of a para-substituted aniline donor, where the para substituents are X = H, OMe, and NMe_2. The imide group of 6ANI is linked to a naphthalene-1,8:4,5-bis(dicarboximide) (NI) electron acceptor across a phenyl spacer in a meta relationship. The triads undergo two-step photoinduced ET to yield their respective XAn$^{\bullet+}$-6ANI-Ph-NI$^{\bullet-}$ RP states. These RPs undergo RP-ISC to yield ^{3}*NI. Application of an external magnetic field, prior to photoexcitation, results in Zeeman splitting of the triplet sublevels, which produces a decrease in the triplet yield if the singlet−triplet splitting of the RP, 2*J*, is small, or a resonance if 2*J* is somewhat larger, due to enhanced singlet−triplet mixing for fields at which level crossing occurs (Figure 1). Structural restrictions in these compounds permit the direct measurement of well-defined 2*J* resonances.[11] The energy of the 2*J* resonance correlates strongly with the distance separating the RPs, r_{DA}, which relates directly to the electronic coupling matrix element for CR, V_{CR}.[19−24] In addition, 2*J* is sensitive to the geometry of the bonding network joining the RPs, thus making it possible to evaluate the dependence of V_{CR} and, thus, ET rates on the details of the RP molecular structure.

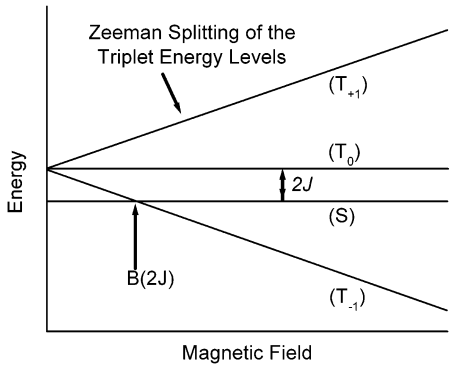

Figure 1. Radical ion pair energy levels as a function of magnetic field.

We now present direct measurements of the RP spin dynamics for the three triads shown in Chart 2, which complement our recent studies of the magnetic field effects on the triplet yield of CR in these systems.[11] These compounds were studied in isotropic toluene solutions, or in partially oriented nematic liquid crystals (LCs), using TREPR spectroscopy. This work builds on our previous TREPR studies of rodlike molecules with a para relationship between 6ANI and the NI acceptor.[7,12] The XAn donor and NI acceptor moieties were chosen for their redox properties and for their clear spectral signatures in time-resolved optical transient absorption measurements,[25−27] while 6ANI was selected because its lowest excited singlet state has a high degree of charge-transfer character and this state can be easily oxidized or reduced.[28]

(11) Lukas, A. S.; Bushard, P. J.; Wasielewski, M. R. *J. Am. Chem. Soc.* **2003**, *125*, 3921−3930.
(12) Weiss, E. A.; Ratner, M. A.; Wasielewski, M. R. *J. Phys. Chem. A* **2003**, in press.
(13) Thurnauer, M. C.; Katz, J. J.; Norris, J. R. *Proc. Natl. Acad. Sci. U.S.A.* **1975**, *72*, 3270.
(14) Dutton, P. L.; Leigh, J. S.; Seibert, M. *Biochem. Biophys. Res. Commun.* **1972**, *46*, 406.
(15) Regev, A.; Nechushtai, R.; Levanon, H.; Thornber, J. P. *J. Phys. Chem.* **1989**, *93*, 2421.
(16) Rutherford, A. W.; Paterson, D. R.; Mullet, J. E. *Biochim. Biophys. Acta* **1981**, *635*, 205.
(17) Kuciauskas, D.; Liddell, P. A.; Moore, A. L.; Moore, T. A.; Gust, D. *J. Am. Chem. Soc.* **1998**, *120*, 10880−10886.
(18) Gilch, P.; Pollinger-Dammer, F.; Musewald, C.; Michel-Beyerle, M. E.; Steiner, U. E. *Science* **1998**, *281*, 982−984.
(19) Anderson, P. W. *Phys. Rev.* **1959**, *115*, 2−13.
(20) Soos, Z. *Annu. Rev. Phys. Chem.* **1974**, *25*, 121−153.
(21) Okamura, M. Y.; Isaacson, R. A.; Feher, G. *Biochim. Biophys. Acta* **1979**, *546*, 394.
(22) Nelsen, S. F.; Ismagilov, R. F.; Teki, Y. *J. Am. Chem. Soc.* **1998**, *120*, 2200−2201.
(23) Kobori, Y.; Sekiguchi, S.; Akiyama, K.; Tero-Kubota, S. *J. Phys. Chem. A* **1999**, *103*, 5416−5424.
(24) Yago, T.; Kobori, Y.; Akiyama, K.; Tero-Kubota, S. *J. Phys. Chem. B* **2002**, *106*, 10074−10081.
(25) Gaines, G. L.; O'Neil, M. P.; Svec, W. A.; Niemczyk, M. P.; Wasielewski, M. R. *J. Am. Chem. Soc.* **1991**, *113*, 719−721.
(26) Hester, R. A.; Williams, K. P. J. *J. Chem. Soc., Perkin Trans. 2* **1982**, *2*, 559.
(27) Viehbeck, A.; Goldberg, M. J.; Kovac, C. A. *J. Electrochem. Soc.* **1990**, *137*, 1460−1466.
(28) Alexiou, M. S.; Tychopoulos, V.; Ghorbanian, S.; Tyman, J. H. P.; Brown, R. G.; Brittain, P. I. *J. Chem. Soc., Perkin Trans. 2* **1990**, *2*, 837−842.

The solvation properties of LCs make them very useful for elucidating ET mechanisms and spin dynamics in donor−acceptor systems.[6,29] This is due to (1) their ability to partially orient the donor−acceptor molecules, making it posible to study the effects of anisotropic media on the ET process; (2) their unique dielectric properties that serve to slow ET rates, making it possible to use the ∼100-ns time resolution of TREPR spectroscopy to investigate ET reactions; and (3) the wide temperature range over which TREPR spectra of RPs and triplet states can be observed in LCs.

Experimental Section

The syntheses of compounds XAn-6ANI-Ph-NI (where X = H, OMe, and NMe_2) are described elsewhere.[11] The solvents used in this study are toluene (Merck Ltd.), which was dried over molecular sieves, and a nematic LC E-7 (Merck Ltd.) with an average dielectric constant of $\epsilon = 19.0$. The solvents are characterized by the following phase transition temperatures:

E-7:

$$\text{crystalline} \xleftrightarrow{210\ \text{K}} \text{soft crystalline} \xleftrightarrow{263\ \text{K}} \text{nematic} \xleftrightarrow{333\ \text{K}} \text{isotropic}$$

toluene:

$$\text{crystalline} \xleftrightarrow{\sim 160\ \text{K}} \text{soft crystalline} \xleftrightarrow{\sim 177\ \text{K}} \text{isotropic}$$

The orientation of the LC director, **L**, with respect to the magnetic field, **B**, is determined by the sign of the diamagnetic susceptibility ($\chi_{\parallel} - \chi_{\perp} = \Delta\chi$). For E-7, $\Delta\chi > 0$; therefore, the default orientation in the fluid phase is **L** || **B**.

At low temperatures (crystalline phase), two sample orientations were studied, **L** || **B** and **L** ⊥ **B**, which may be obtained by rotation of the sample in the microwave resonator by $\pi/2$ about an axis perpendicular to the external magnetic field. In the fluid phase, at higher temperatures (soft crystalline and nematic phases), only the **L** || **B** orientation is obtained, because at these temperatures, where molecular motion is allowed, rotation of the sample has no effect due to the fast molecular reorientation back to the initial parallel configuration. For the preparation of the samples in the LC, the compounds were first dissolved in toluene (∼1 mM), which was then evaporated, and the LC was introduced into 4-mm-o.d. Pyrex tubes. The samples were degassed on a vacuum line by several freeze−pump−thaw cycles. TREPR measurements were carried out on a Bruker ESP-380 CW spectrometer with the field modulation disconnected as described elsewhere.[30] Temperatures were maintained by using a variable-temperature nitrogen flow dewar in the EPR resonator. The samples were photoexcited at 420 nm (∼4 mJ/pulse at a repetition rate of 10 Hz) by a Continuum Panther OPO laser pumped by the third harmonic of a Continuum Surelite SLII-10 laser. This wavelength corresponds to the absorption wavelength of the 6ANI moiety in XAn-6ANI-Ph-NI.

Analysis of the TREPR spectra of the photoexcited triplets oriented in different matrices, i.e., isotropic and uniaxial LC, is described in detail elsewhere.[31,32] The extracted zero-field splitting (ZFS) parameters, $|D|$ and $|E|$, and the corresponding relative triplet population rates, A_x, A_y, and A_z, are given in Table 1. The definition of molecular axes and angles with respect to the director, **L**, is given in Figure 2. The preferred in-plane orientation of the guest molecules, with respect to **L**, is given by the angle ϕ_0 with the variance σ_ϕ. The angle θ' describes the fluctuations of the averaged molecular plane about **L** with a variance $\sigma_{\theta'}$.

(29) Greenfield, S. R.; Svec, W. A.; Wasielewski, M. R.; Hasharoni, K.; Levanon, H. In *The Reaction Center of Photosynthetic Bacteria*; Michel-Beyerle, M.-E., Ed.; Springer: New York, 1996; pp 81−87.
(30) Berg, A.; Galili, T.; Kotlyar, A. B.; Hazani, M.; Levanon, H. *J. Phys. Chem. A* **1999**, *103*, 8372−8374.
(31) Gonen, O.; Levanon, H. *J. Chem. Phys.* **1986**, *84*, 4132−4141.
(32) Regev, A.; Galili, T.; Levanon, H. *J. Phys. Chem.* **1996**, *100*, 18502−18510.

Table 1. Parameters Obtained from TREPR Experiments on XAn-6ANI-Ph-NI

XAn	solvent	T (K)	$\lvert D\rvert^a$	$\lvert E\rvert^a$	A_x:A_y:A_z	$\sigma_{\theta'}{}^b$	$\varphi_0{}^b$	$\sigma_{\varphi 0}{}^b$
HAn	toluene	135	696.3	7.5	1:1:1[c]			
HAn	E-7	170	696.3	7.5	1:1:1[c]	35	60	5
MeOAn	toluene	135	696.3	7.5	1:1:1[c]			
MeOAn	E-7	170	696.3	11.2	1:1:1[c]	30	50	5
Me_2NAn[e]	E-7	170	696.3	7.5	0.8:0.2:0.0[d]	30	65	10

[a] $\times 10^4$ cm^{-1}, uncertainty 10%. [b] In degrees, uncertainty 10%. [c] Through S−T_0 mixing mechanism. [d] Through S−T_0 and S−T_{-1} mixing mechanisms. [e] When the donor is Me_2NAn, no TREPR spectra are observed in toluene.

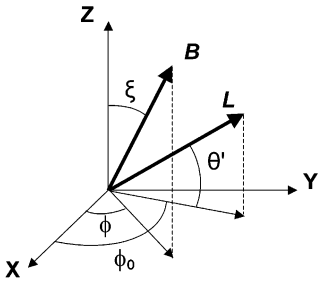

Figure 2. Molecular frame of reference (*X*,*Y*,*Z*) and its relationship to the magnetic field, **B**, and the director of the LC, **L**, defined in the laboratory axis frame.

Results and Discussion

TREPR Spectra in Toluene. Compounds HAn-6ANI-Ph-NI and MeOAn-6ANI-Ph-NI dissolved in toluene exhibit TREPR spectra over a wide range of temperatures (135−300 K). However, Me_2NAn-6ANI-Ph-NI dissolved in toluene shows no TREPR spectrum. The spectra at 135 K are shown in Figure 3. Both HAn-6ANI-Ph-NI and MeOAn-6ANI-Ph-NI exhibit a broad spectrum with a width of ∼150 mT and a polarization pattern (a,e,e,a,a,e*)* (from low to high field; a stands for absorption and e for emission).

In the case of HAn-6ANI-Ph-NI, at 150 K an additional spectral feature appears, namely, a narrow spectrum at $g \approx 2$, superimposed on the broad one. The phase pattern of this narrow signal is time dependent, as shown clearly in Figure 4. The superposition of the two spectra persists up to ∼180 K, and above it the triplet spectrum disappears, while the narrow signal is still observable. The same trend is observed for MeOAn-6ANI-Ph-NI, except that the superimposed narrow signal appears at 135 K, and the triplet spectrum disappears at ∼170 K. As was already mentioned, Me_2NAn-6ANI-Ph-NI does not exhibit any signal in toluene in the temperature range of 135−300 K.

The broad spectra are assigned to HAn-6ANI-Ph-^{3}*NI and MeOAn-6ANI-Ph-^{3}*NI and, except for their phase patterns, are identical to the spectrum of ^{3}*NI alone.[7,9,10] The positions of the *X*, *Y*, and *Z* canonical orientations and ZFS parameters support this assignment. As will be discussed later, the narrow signal superimposed on the broad spectra is attributed to the radical pair $XAn^{\bullet+}$-6ANI-Ph-$NI^{\bullet-}$.

The results of the line shape analysis of the broad triplet spectra, taken at low temperature in toluene (135 K), are presented in Table 1. The unique and unusual line shape pattern (a,e,e,a,a,e) of the triplet spectra of HAn-6ANI-Ph-^{3}*NI and MeOAn-6ANI-Ph-^{3}*NI indicates unambiguously that such a polarization pattern cannot be generated by spin−orbit intersystem crossing (SO-ISC). Such a pattern is typical of RP-ISC, where the high-field triplet sublevel, T_0, is overpopulated in all

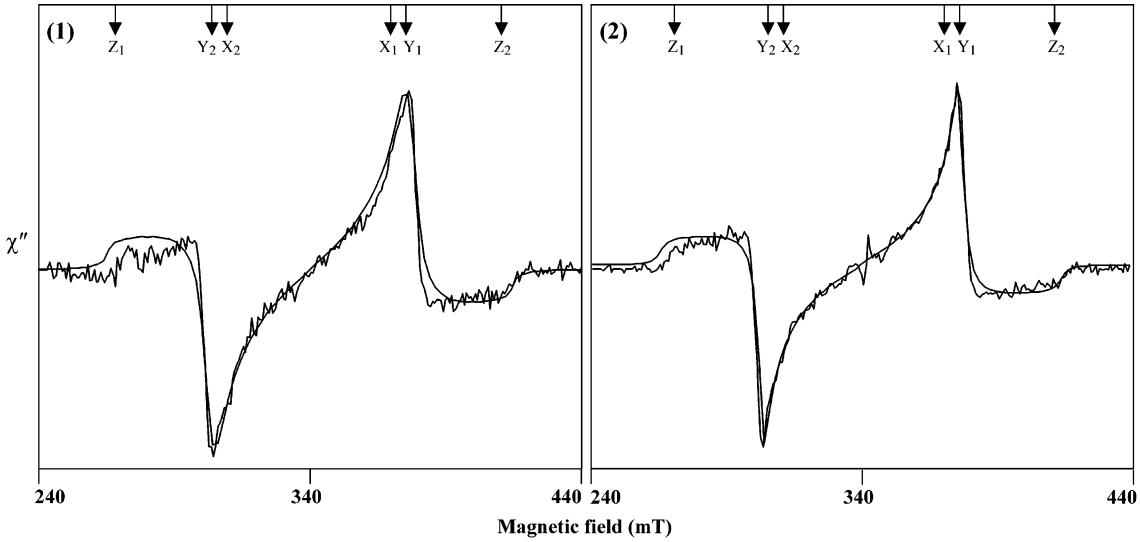

Figure 3. TREPR spectra of HAn-6ANI-Ph-NI **(1)** and MeOAn-6ANI-Ph-NI **(2)** (triplets and RPs), dissolved in toluene at 135 K. Spectra were taken 0.6 μs after laser pulse at 420 nm photoexcitation (4 mJ/pulse). Smooth curves superimposed on the experimental spectra are triplet computer simulations with the parameters given in Table 1. The canonical orientations are indicated by arrows at the top of each spectrum.

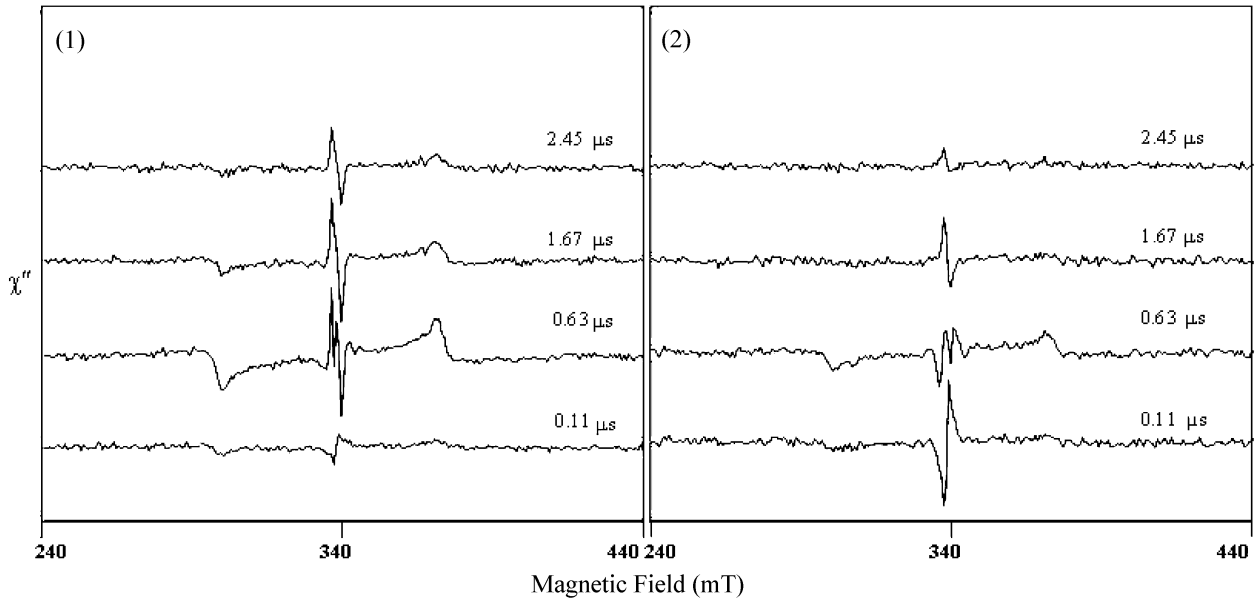

Figure 4. TREPR spectra at 150 K (triplets and RPs) of HAn-6ANI-Ph-NI **(1)** and MeOAn-6ANI-Ph-NI **(2)**, dissolved in toluene, at different times after laser pulse (420 nm, 4 mJ/pulse).

canonical orientations (S−T_0 mixing). Indeed, the triplet spectra of HAn-6ANI-Ph-^{3}*NI and MeOAn-6ANI-Ph-^{3}*NI could be simulated by applying an S−T_0 mixing mechanism, corrected for the faster disappearance of signal intensity at the *z* orientation of the triplet, i.e., anisotropic spin lattice relaxation (SLR).

Thus, the broad triplet spectra of HAn-6ANI-Ph-^{3}*NI and MeOAn-6ANI-Ph-^{3}*NI in toluene are formed via RP-ISC mechanism, in accordance with the energy level diagram in Figure 5. Selective photoexcitation of 6ANI generates the excited singlet state, which accepts an electron from HAn or MeOAn. This initial ET produces the primary RP, ^{1}[XAn$^{\bullet+}$-6ANI$^{\bullet-}$-Ph-NI]. A secondary, thermal ET produces ^{1}[XAn$^{\bullet+}$-6ANI-Ph-NI$^{\bullet-}$], which undergoes S−T mixing to yield ^{3}[XAn$^{\bullet+}$-6ANI-Ph-NI$^{\bullet-}$]. This process is associated with the narrow spectrum superimposed on the broad triplet spectrum of XAn-6ANI-Ph-^{3}*NI, generated by charge recombination within ^{3}[XAn$^{\bullet+}$-6ANI-Ph-NI$^{\bullet-}$], via RP-ISC.

TREPR Spectra in E-7. All three compounds, dissolved in E-7, exhibit TREPR spectra over a wide temperature range. The ordered spectra in the crystalline phase at 170 K are shown in Figure 6. HAn-6ANI-Ph-^{3}*NI exhibits a broad polarized spectrum having a pattern of (a,e,e,a,a,e), together with a very weak, narrow (e,a) signal at the central part of the spectrum. This narrow signal will be discussed in detail in the next section. As indicated above, at elevated temperatures only the **L** || **B** spectra can be recorded. The broad triplet spectrum appears to weaken with increasing temperature and could be observed up to 270 K (Figure 7).

On the other hand, the narrow signal intensifies in the soft glass phase and persists up to 320 K. It also exhibits time-dependent polarization patterns, i.e., (e,a) at early times, changing into (a,e) at later times. The phase inversion region depends on the temperature (Figure 8). The broad triplet spectrum of MeOAn-6ANI-Ph-^{3}*NI at 170 K is similar to that

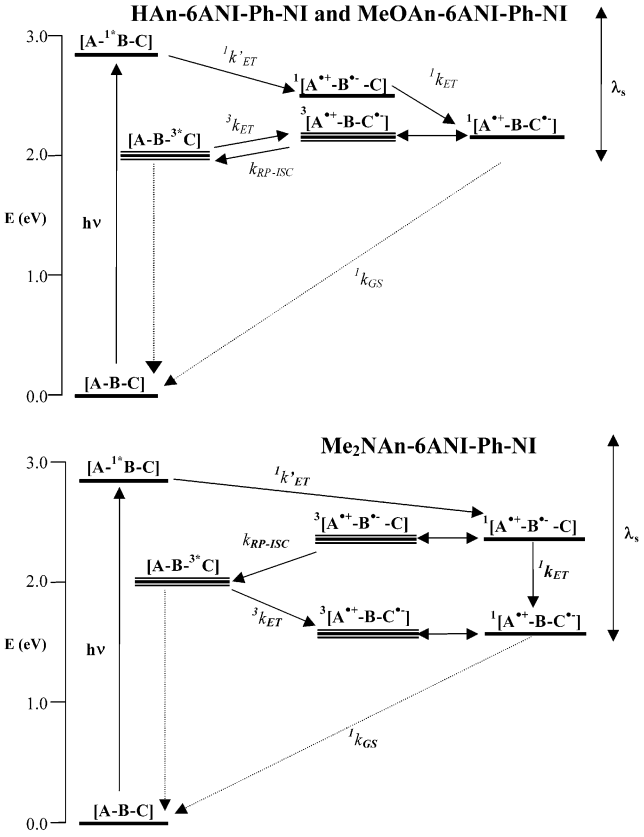

Figure 5. Energy level diagrams for the indicated compounds. The triad components are abbreviated as A, B, and C. The temperature-dependent solvent reorganization energy is represented by λ_S.

of HAn-6ANI-Ph-^{3}*NI and shows a (a,e,e,a,a,e) polarization pattern (Figure 6), but with a considerably better signal-to-noise ratio. The same holds for the narrow spectrum, which is much stronger than that for HAn-6ANI-Ph-NI. This strong, narrow spectrum has a general polarization pattern (e,a) in both **L** || **B** and **L** ⊥ **B** configurations. The triplet spectrum of MeOAn-6ANI-Ph-^{3}*NI disappears at 250 K (Figure 7), while the narrow signal persists up to 310 K. Also in this case, the narrow signal changes its phase from (e,a) to (a,e) as a function of time (Figure 8).

Line shape analysis of the triplet spectra of HAn-6ANI-Ph-^{3}*NI and MeOAn-6ANI-Ph-^{3}*NI in E-7 was based on the analysis of their spectra in toluene. Also here, the spectral line shape is typical of S−T_0 mixing mechanism, combined with anisotropic SLR. In addition, orientational parameters were found, characterizing the alignment of HAn-6ANI-Ph-^{3}*NI and MeOAn-6ANI-Ph-^{3}*NI with respect to **L** (Table 1). These results suggest that the molecules do not align parallel to the director **L**. This is indicated by a relatively large value of $\sigma_{\theta'} \approx 30°$ (Figure 9). The $\sigma_{\theta'}$ value is in line with the molecular structures of HAn-6ANI-Ph-^{3}*NI and MeOAn-6ANI-Ph-^{3}*NI (Chart 2). The values found for ϕ_0 (∼60°), which determine the most probable location of **L** in the molecular plane, show that the planes of NI are tilted relative to **L**. It is noteworthy that such a tilted orientation of NI, characterized by large values of ϕ_0, was found in other covalently linked donor−acceptor systems of different geometries, containing NI, in a rodlike system.[7] From the present results, it seems that the interaction of the C_8H_{17} aliphatic tail with the LC dominates, resulting in its preferential alignment along the LC director, which in turn forces the molecular plane of NI to be 30° to **L**.

As was mentioned above, Me_2NAn-6ANI-Ph-NI does not exhibit any TREPR signals in toluene at any temperature. Moreover, Me_2NAn-6ANI-Ph-NI does not exhibit a magnetic field effect (MFE) in toluene at 295 K,[11] because the energy of $Me_2NAn^{\bullet+}$-6ANI-Ph-$NI^{\bullet-}$ is below that of Me_2NAn-6ANI-Ph-^{3}*NI.[11] While significant S−T mixing is likely to occur within $Me_2NAn^{\bullet+}$-6ANI-Ph-$NI^{\bullet-}$ due to the ∼20-Å distance between

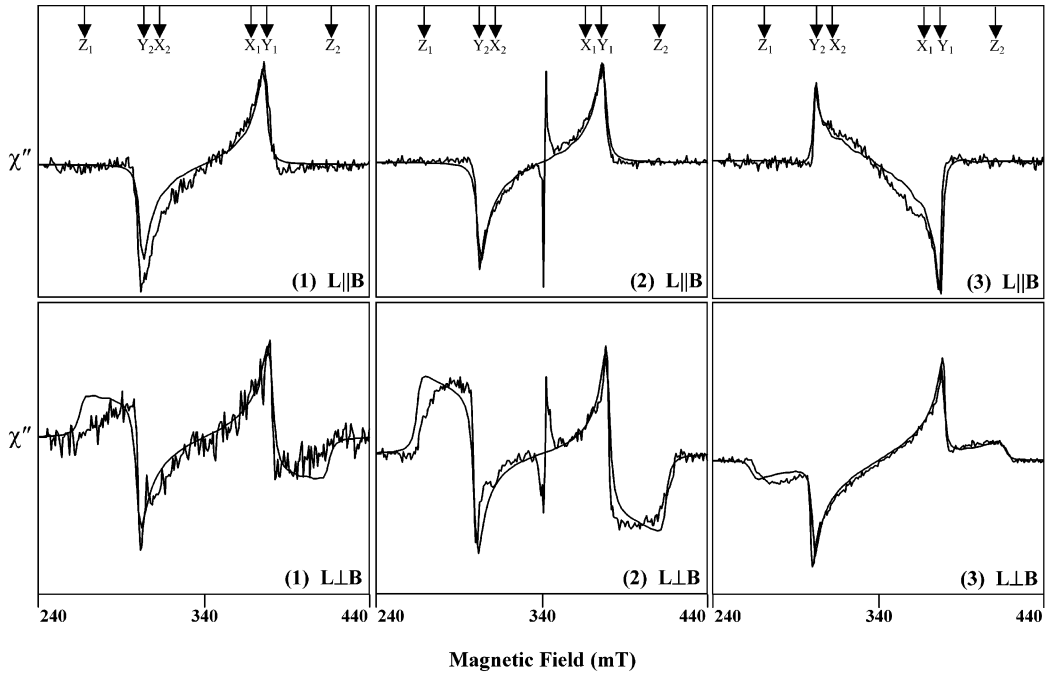

Figure 6. TREPR spectra of HAn-6ANI-Ph-NI, MeOAn-6ANI-Ph-NI, and Me_2NAn-6ANI-Ph-NI (**1**, **2**, and **3**, respectively; triplets and RPs), dissolved in E-7, in **L** || **B** and **L** ⊥ **B** configurations, at 170 K. All other experimental conditions are as in Figure 3. Smooth curves superimposed on the experimental spectra are triplet computer simulations with the parameters given in Table 1. The canonical orientations are indicated by arrows at the top of each spectrum.

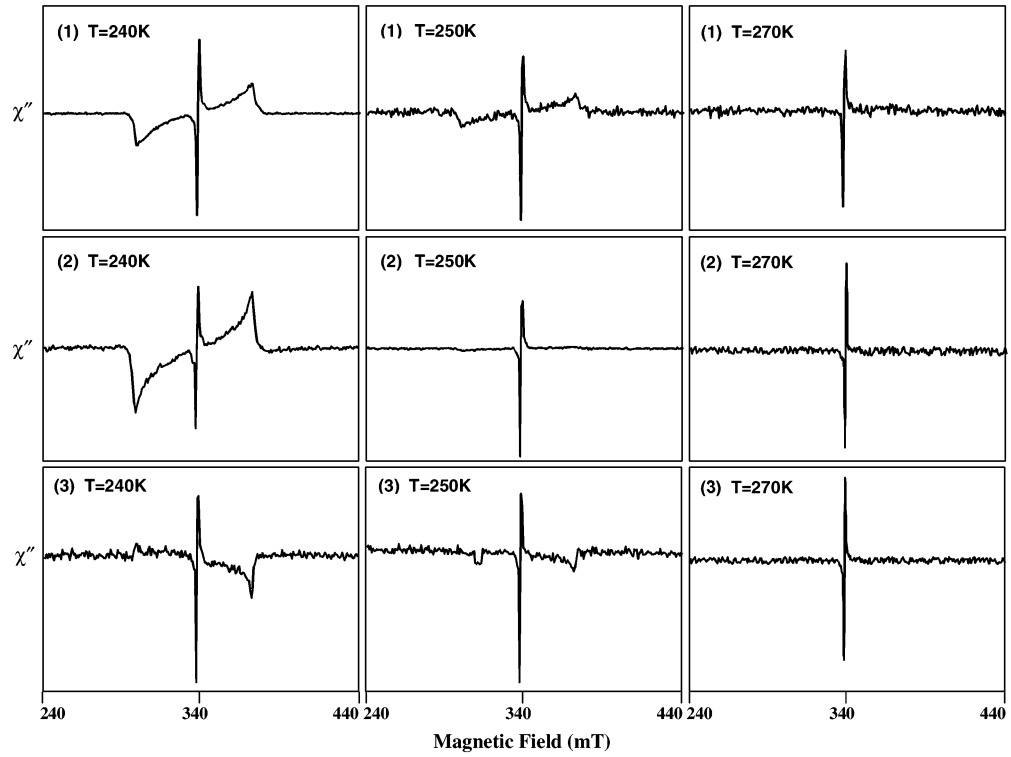

Figure 7. TREPR spectra of HAn-6ANI-Ph-NI, MeOAn-6ANI-Ph-NI, and Me2NAn-6ANI-Ph-NI (**1**, **2**, and **3**, respectively; triplets and RPs), dissolved in E-7, in **L** || **B** configuration, at different temperatures. All other experimental conditions are as given in Figure 3.

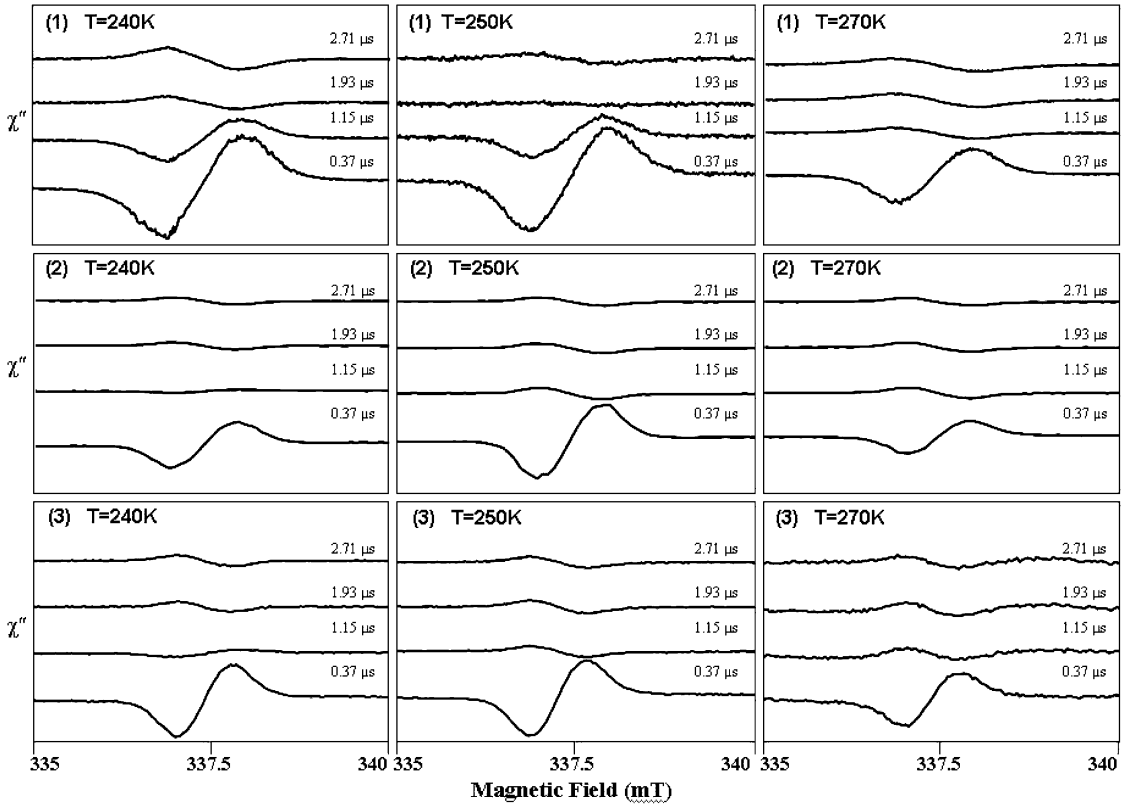

Figure 8. TREPR spectra of HAn-6ANI-Ph-NI, MeOAn-6ANI-Ph-NI, and Me_2NAn-6ANI-Ph-NI (**1**, **2**, and **3**, respectively), dissolved in E-7, in **L** || **B** configuration, at different temperatures and different times after the 420 nm, 4 mJ laser pulse. All other experimental conditions are as in Figure 3.

the radicals, CR from the singlet RP occurs directly to the ground state. In the LC, however, the broad and narrow spectra are observed over a wide range of temperatures. The oriented triplet spectra were recorded at 170 K, with a spectral width and field positions of the canonical orientations similar to those recorded for HAn-6ANI-Ph-^{3}*NI and MeOAn-6ANI-Ph-^{3}*NI. Thus, for Me_2NAn-6ANI-Ph-NI, the observed broad triplet signal is also assigned to ^{3}*NI. However, the triplet spectrum

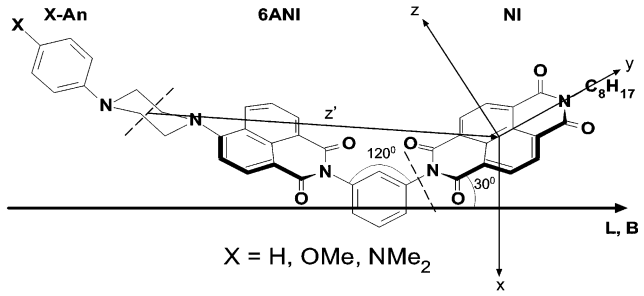

Figure 9. Schematic presentation of the molecular structure of the XAn-6ANI-Ph-NI triad system and its orientation in E-7. The molecular axes (*X*,*Y*,*Z*) are presented for NI. The 30° angle between the NI molecular plane and **L** was deduced from line shape analysis of [XAn-6ANI-Ph-^{3}*NI]. The angle of 120° between 6ANI and NI is defined by their meta linkage to the phenyl bridge. *z*′ is the RP dipolar axis. The angle ξ between *z*′ and **B** is not shown due to its small value.

of Me_2NAn-6ANI-Ph-^{3}*NI has a polarization pattern which is different from those of HAn-6ANI-Ph-^{3}*NI and MeOAn-6ANI-Ph-^{3}*NI, namely, (e,e,a,e,a,a) (Figure 6). Also here, the triplet spectrum is accompanied by a narrow, weak signal, which will be discussed in the next section. In the case of Me_2NAn-6ANI-Ph-NI, the broad triplet spectrum disappears at 260 K (Figure 7), while the narrow signal is observed up to 330 K, changing its phase pattern from (e,a) to (a,e) as a function of time (Figure 8).

The results of the line shape analysis are presented in Table 1, and warrant some further discussion. Inspection of the TREPR spectrum of Me_2NAn-6ANI-Ph-^{3}*NI in Figure 6 shows that the observed polarization pattern, (e,e,a,e,a,a), is not consistent with either the $S-T_0$ or $S-T_{-1}$ mixing mechanisms. It is also different from the polarization pattern of the triplet spectrum of the monomer NI.[7,9,10] Such a polarization pattern was previously reported for covalently linked RPs containing the NI acceptor that have short distances between the radical ions.[9,10] Such an unusual line shape was explained in terms of both $S-T_0$ and $S-T_{-1}$ mixing mechanisms, which may be operative simultaneously in RPs for which *J* is relatively large. Thus, we propose that a different RP is responsible for the observed TREPR spectra. In analyzing the "unusual" line shape pattern, one should recall that the triplet spectra in the RP systems with short radical ion distances are identical to the triplet spectrum of Me_2NAn-6ANI-Ph-^{3}*NI obtained here.[9,10] This implies that the observed triplet spectrum is generated by CR of the primary RP, i.e., $Me_2NAn^{\bullet+}$-$6ANI^{\bullet-}$-Ph-NI. In such a "short-distance" RP, the value of *J* should be significantly higher than that of the secondary RP, thus permitting $S-T_{-1}$ mixing. However, it is evident that the lifetime of the primary RP is too short to allow for its direct observation by TREPR (time resolution of ~100 ns). This implies that the narrow observed signal should be attributed to the relatively long-lived secondary RP, $Me_2NAn^{\bullet+}$-6ANI-Ph-$NI^{\bullet-}$. Thus, the primary RP $Me_2NAn^{\bullet+}$-$6ANI^{\bullet-}$-Ph-NI decays by two parallel channels to yield $Me_2NAn^{\bullet+}$-6ANI-Ph-$NI^{\bullet-}$ and Me_2NAn-6ANI-Ph-^{3}*NI. This is a consequence of positioning the energy level of Me_2NAn-6ANI-Ph-^{3}*NI between those of $Me_2NAn^{\bullet+}$-$6ANI^{\bullet-}$-Ph-NI and $Me_2NAn^{\bullet+}$-6ANI-Ph-$NI^{\bullet-}$, as is seen in Figure 5, and is discussed further below.

Radical Pair Spectra. The narrow spectra superimposed on the broad triplet spectra can be attributed either to a CRP or to a TRP. Both mechanisms have been treated previously at length.[7,33−35] While the CRP is governed by the dipolar (*D*) and the spin−spin exchange (*J*) interactions, the TRP is governed by the dipolar interaction only (in such a case, $J \gg D$). RPs may be generated from either singlet or triplet precursors, where the phase pattern of the RP spectrum shows whether the RP is generated by a singlet or a triplet precursor ($^1k_{ET}$ or $^3k_{ET}$, respectively, in Figure 5).

TRP was observed previously in covalently linked systems with short donor−acceptor distances of ~11 Å, where single-step ET occurs.[9,10,35] In covalently linked systems, in which two-step ET leads to longer donor−acceptor distances (~18−24 Å), the observed long-distance RPs were found to be spin-correlated via the CRP mechanism.[7,35] Without taking into account hyperfine interactions, the CRP spectrum consists of two antiphase doublets, centered at the *g*-factor of the individual radicals of the pair. The splitting in each doublet is determined by *J* and *D*. Resolved hyperfine interactions lead to further splitting of the doublet for each radical. The experimentally observed CRP spectrum is a superposition of the four-line spectra for all possible orientations of the RP, with respect to the external magnetic field, **B**. The positions (ω_{ij}) of the four EPR transitions for CRP are[36,37]

$$\begin{aligned}\omega_{12} &= \omega_0 - \Omega - J + D_{zz}\\ \omega_{34} &= \omega_0 - \Omega + J - D_{zz}\\ \omega_{13} &= \omega_0 + \Omega - J + D_{zz}\\ \omega_{24} &= \omega_0 + \Omega + J - D_{zz}\end{aligned} \qquad (1)$$

where ω_0 is the center of the spectrum and

$$\Omega^2 = (J + D_{zz}/2)^2 + Q^2$$

$$Q = {}^1/_2(g_1 - g_2)\mu\hbar^{-1}B_0 + {}^1/_2(\sum_i a_{1i}m_{1i} - \sum_j a_{2j}m_{2j}) \qquad (2)$$

$$D_{zz} = D[\cos^2(\xi) - 1/3]$$

where ξ is the angle between the dipolar axis (z′ in Figure 9) and the magnetic field direction, **B**.

The phase of the EPR signal is determined by the CRP sign rule,[7]

$$\Gamma = -\mu\cdot\mathrm{sign}\{J + D[3\cos^2(\xi) - 1]\} = \begin{cases} -e/a \\ +a/e \end{cases} \qquad (3)$$

where μ is −1 or +1 for a singlet or a triplet precursor, respectively.

Line shape analysis of the triplet spectra of XAn-6ANI-Ph-^{3}*NI reveals the molecular orientation of the triad with respect to **L** and **B** (Figure 9). This analysis results in a value of ~30° for θ', which is the angle between the plane of NI and the director **L**. The ~120° angle between the XAn and NI moieties, held together via the benzene ring through the meta connection, was confirmed by AM1 molecular orbital calculations of the

(33) Hasharoni, K.; Levanon, H.; von Gersdorff, J.; Kurreck, H.; Mobius, K. *J. Chem. Phys.* **1993**, *98*, 2916−2926.
(34) Levanon, H.; Hasharoni, K. *Prog. React. Kinet.* **1995**, *20*, 309−346.
(35) Levanon, H.; Galili, T.; Regev, A.; Wiederrecht, G. P.; Svec, W.; Wasielewski, M. R. *J. Am. Chem. Soc.* **1998**, *120*, 6366−6373.
(36) Norris, J. R. M.; Thurnauer, A. L.; Tang, M. C. J. *J. Chem. Phys.* **1990**, *92*, 4239−4249.
(37) Hore, P. J. *Analysis of Polarized EPR Spectra*; Elsevier: Amsterdam, 1989.

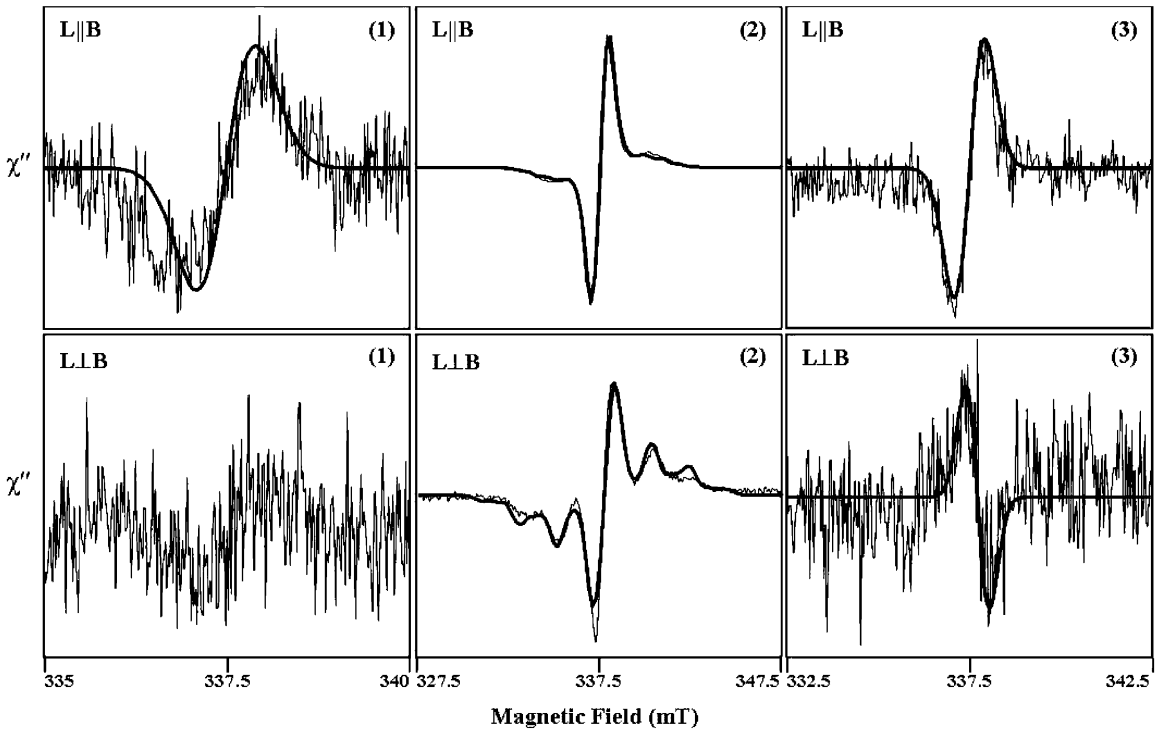

Figure 10. TREPR spectra of HAn-6ANI-Ph-NI, MeOAn-6ANI-Ph-NI, and Me_2NAn-6ANI-Ph-NI (**1**, **2**, and **3**, respectively), dissolved in E-7, at 170 K. Other experimental conditions are as in Figure 3. Smooth curves superimposed on the experimental spectra are computer simulations (eqs 1 and 2) with parameters presented in Tables 2 and 3. Note that the simulation of the **L** ⊥ **B** spectrum of **1** was not done due to the poor signal-to-noise ratio of the experimental spectrum.

energy-minimized geometry.[38] Inspection of Figure 9 shows that the angle between the dipolar axis, z', and the magnetic field direction, **B**, calculated from the molecular structure, is very small ($\xi \approx 9°$). In the case of head-to-tail spin orientation, $D < 0$, and by assuming $J < 0$, the observed phase pattern (e,a), at early times in all three compounds (**L** || **B** configuration), yields a negative Γ (Figure 10). In terms of eq 3, this phase pattern corresponds to a singlet precursor to the RPs, in full agreement with the proposed electron-transfer mechanism (Figure 5). At high temperatures, the change of the phase pattern at later times to (a,e) (Figure 8) indicates that XAn-6ANI-Ph-^{3}*NI is the RP precursor to generate the CRP with a rate constant of $^3k_{ET}$. To summarize, in all three triads studied here, the final product is the CRP.

Upon sample rotation at low temperatures (crystalline phase) from **L** || **B** to **L** ⊥ **B**, the dipolar angle ξ in eq 3 should be replaced by ($\xi + 90°$). This, in principle, can change the sign of Γ and results in a spectral phase change from (e,a) to (a,e) for the same precursor.[7,35] Such a phase change was not observed in HAn-6ANI-Ph-NI and MeOAn-6ANI-Ph-NI but was observed for Me_2NAn-6ANI-Ph-NI (Figures 6 and 10). It is noteworthy that, although the RP signal of HAn-6ANI-Ph-NI at 170 K is very weak, the phase patterns for **L** || **B** and **L** ⊥ **B** can be determined unambiguously (Figure 10). The RP signal of MeOAn-6ANI-Ph-NI, however, exhibits a good signal-to-noise ratio. It consists of a strong, narrow doublet in the center and, superimposed on it, a structured signal (Figure 10), which will be discussed in detail below.

From eq 3, it is evident that, for $J > \{D[3\cos^2(\xi) - 1]\}$, the sign of Γ does not change upon changing ξ to ($\xi + 90°$), thus preserving the RP's phase pattern. Thus, if HAn-6ANI-Ph-NI and MeOAn-6ANI-Ph-NI fulfill the above requirement, then no phase change is expected upon sample rotation. On the other hand, Me_2NAn-6ANI-Ph-NI exhibits a phase change upon sample rotation, leading to the conclusion that $J < \{D[3\cos^2(\xi) - 1]\}$.

Table 2. Dipolar and Exchange Couplings Extracted from the Line Shape Analysis of the Correlated Radical Pairs within XAn-6ANI-Ph-NI

XAn in XAn$^{\bullet+}$-6ANI-Ph-NI$^{\bullet-}$	D^a (mT)	J^a (mT)	r^b(Å)	$\lvert J\rvert^c$ (mT)	r^f (Å)
HAn	−1.1	−0.9	17	26.2	17.4
MeOAn	−0.8	−0.6	19	0.75[d]	19.3[d]
				7.5[e]	18.2[e]
Me_2NAn	−0.63	0	20.5		20.1

[a] Obtained by line shape analysis of RPs spectra, uncertainty ±10%. [b] As estimated from D values, obtained through line shape analysis and presented in this table. [c] As obtained by MFE measurements, uncertainty ± 5%. [d] For chair conformation. [e] For boat conformation. [f] As obtained from spin density calculations.

The CRP spectra of all three triads were simulated using the expressions given by eqs 1 and 2, with the best-fit parameters summarized in Tables 2 and 3. Generally, simulations of the CRP spectra require knowledge of the g-factors (or Δg), hyperfine splitting constants, a_H and a_N, and J and D values. Not all of these parameters are available for the triads. The g-factor and hyperfine constants of related radicals, such as the *N*,*N*-diphenyl derivative of NI$^{\bullet-}$ and the *N*,*N*-dimethyl-*p*-anisidine radical cation, were used in the simulations.[39−43]

(38) AM1 calculations were performed using HyperChem, Hypercube, Inc., 1115 NW 1114th St., Gainesville, FL 32601.

(39) Heinen, U.; Berthold, T.; Kothe, G.; Stavitski, E.; Galili, T.; Levanon, H.; Wiederrecht, G.; Wasielewski, M. R. *J. Phys. Chem. A* **2002**, *106*, 1933−1937.

(40) Ciminale, F.; Curci, R.; Portacci, M.; Troisi, L. *Tetrahedron Lett.* **1988**, *29*, 2463−2466.

Table 3. Parameters Used in Line Shape Analysis of the Correlated Radical Pairs

	g-factor	a_N (mT)	a_H (mT)
$NI^{\bullet-}$	2.0031[a]	0.1 (×2)[a]	0.19 (×4)[a]
p-$MeOAn^{\bullet+}$	2.003 ± 0.0005[b]	1.5 (×1)[b]	0.5 (×2)[b,c]
			0.6 (×4)[b,d]

[a] Values estimated on the basis of published data for related radicals, as indicated in the text. [b] Values used in simulation of the correlated radical pair spectrum of MeOAn-6ANI-Ph-NI (this work). [c] For ortho protons. [d] For methylene protons.

Within this context, only MeOAn-6ANI-Ph-NI exhibits a structured spectrum which could be simulated. Regarding $MeOAn^{\bullet+}$, its *g*-factor and hyperfine constants a_N and a_H were determined by the line shape simulations and are given in Table 3. These results are very close to those obtained for related compounds, such as the *N*,*N*-dimethyl-*p*-anisidine radical cation,[40] aniline,[44] and Wurster's blue[45,46] radicals. The $MeOAn^{\bullet+}$ contribution to the overall CRP spectrum of MeOAn-6ANI-Ph-NI is still present in the soft glass phase of LC but disappears at higher temperatures in the nematic phase, due to line broadening. The absence of the $XAn^{\cdot+}$ contribution in the RP spectra of HAn-6ANI-Ph-NI and Me_2NAn-6ANI-Ph-NI may be explained by the poor signal-to-noise ratio. From the *D* values, obtained by the line shape analysis, the effective RP distances, **r**, were estimated through the dipole−dipole approximation,

$$|D| \cong {}^3/_4(g\beta)^2/r^3 \qquad (4)$$

and they are given in Table 2. A structured spectrum was observed previously in the CRP spectrum of a porphyrin-based photosynthetic model system.[45] In this system, an initial photoinduced electron transfer produced a zinc porphyrin cation−naphthoquinone anion radical pair. This was followed by a thermal reaction in which an *N*,*N*,*N*′,*N*′-tetramethylphenylenediamine (TMPD), rigidly attached to the porphyrin, was oxidized by the zinc porphyrin radical cation to give $TMPD^{\cdot+}$, which yielded the structured spectrum.

It is useful to compare the values of *J* obtained from our magnetic field effect data to those obtained from the spectral fitting procedure described above. Referring to Table 2, the TREPR spectra presented here show that $J = -0.9$ mT for $HAn^{\bullet+}$-6ANI-Ph-$NI^{\bullet-}$, while that obtained from the MFE data is $|J| = 26.2$ mT. On the other hand, the TREPR results for $MeOAn^{\bullet+}$-6ANI-Ph-$NI^{\bullet-}$ yield $J = -0.6$ mT, while the MFE data show two resonances at $|J| = 0.75$ and 7.5 mT. The MFE data cannot determine the sign of *J*, so the sign will be ignored in the following discussion. We showed earlier that the most likely source of the two resonances with $MeOAn^{\bullet+}$-6ANI-Ph-$NI^{\bullet-}$ are the two conformations of the piperazine ring that are illustrated in Figure 11. Structure A shows the chair conformation of the piperazine, in which the two radicals in the pair are about 1.1 Å farther apart than in the B or boat conformation. In

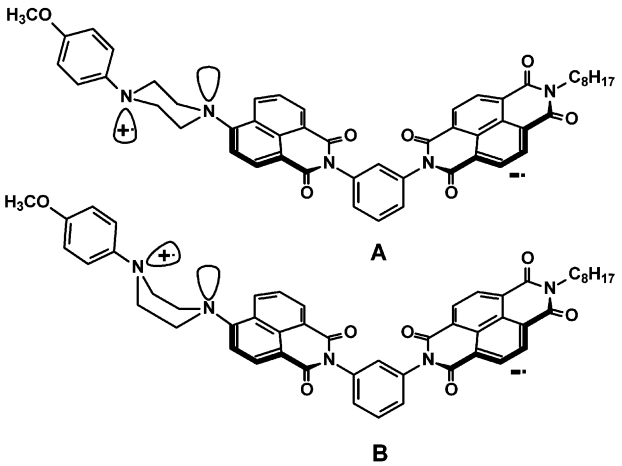

Figure 11. Two conformations of $MeOAn^{+}$-6ANI-Ph-NI^{-} resulting from chair−boat inversion of the piperazine ring.

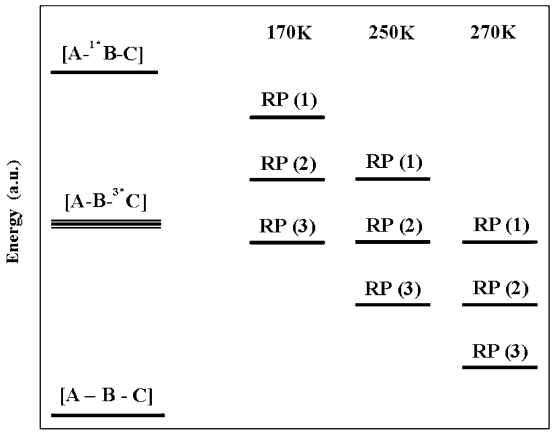

Figure 12. Schematic presentation (not to scale) of the energy levels of the RPs of HAn-6ANI-Ph-NI, MeOAn-6ANI-Ph-NI, and Me_2NAn-6ANI-Ph-NI (**1**, **2**, and **3**, respectively), abbreviated to A, B, and C, at different temperatures, as determined by TREPR data.

toluene at 295 K, the Coulombic attraction of the two charges stabilizes the closer boat conformation through what Verhoeven has termed a "harpooning effect".[47] This effect is accentuated somewhat for $HAn^{\bullet+}$-6ANI-Ph-$NI^{\bullet-}$ in toluene at 295 K, because the distance between the RP spin distributions within this RP is somewhat shorter and the 2*J* resonance is broader, which masks the presence of two resonances due to the chair and boat conformations. Interestingly, the values of *J* decrease significantly in the TREPR spectra obtained in the LC. It is likely that the local order of the nematic LC enforces the chair conformation of each $XAn^{\bullet+}$-6ANI-Ph-$NI^{\bullet-}$ RP, which reduces *J* to about 1 mT in each case.

In Figure 12, we summarize the dependence of the RPs energies in the LC on temperature. Changes in the solvent reorganization energy (λ_s in Figure 5) allow the energies of the RP states to be tuned over a wide range by changing the temperature. Thus, the relative position of the energy levels of the $XAn^{\bullet+}$-6ANI-Ph-$NI^{\bullet-}$ and of XAn-6ANI-Ph-^{3}*NI explains both the absence and the appearance of these two spectra. At 170 K, the energy level of $HAn^{\bullet+}$-6ANI-Ph-$NI^{\bullet-}$ should lie considerably higher than that of its triplet state HAn-6ANI-Ph-^{3}*NI. Therefore, a high driving force allows for an efficient

(41) Kiefer, A. M.; Kast, S. M.; Wasielewski, M. R.; Laukermann, K.; Kothe, G. *J. Am. Chem. Soc.* **1999**, *121*, 188−198.
(42) Zhong, C. J.; Kwan, W. S. V.; Miller, L. L. *Chem. Mater.* **1992**, *4*, 1423−1428.
(43) Nelsen, S. F. *J. Am. Chem. Soc.* **1967**, *89*, 5925.
(44) Neugebauer, F. A. B., S.; Groh, W. R. *Tetrahedron Lett.* **1973**, *25*, 2247−2248.
(45) Laukenmann, K.; Weber, S.; Kothe, G.; Oesterle, C.; Angerhofer, A.; Wasielewski, M. R.; Svec, W. A.; Norris, J. R. *J. Phys. Chem.* **1995**, *99*, 4324−4329.
(46) Kirste, B. *Magn. Reson. Chem.* **1987**, *25*, 166−175.
(47) Lauteslager, X. Y.; van Stokkum, I. H. M.; van Ramesdonk, H. J.; Brouwer, A. M.; Verhoeven, J. W. *J. Phys. Chem. A* **1999**, *103*, 653−659.

CR (k_{RP-ISC}) to produce HAn-6ANI-Ph-^{3}*NI in a high yield. The energy level of MeOAn$^{\bullet+}$-6ANI-Ph-NI$^{\bullet-}$ at this temperature lies lower than that of HAn$^{\bullet+}$-6ANI-Ph-NI$^{\bullet-}$ relative to its triplet energy level. This implies less efficient driving force for the RP-ISC, and so both signals (RP and triplet) are observed simultaneously. At 240 K, the energy level of HAn$^{\bullet+}$-6ANI-Ph-NI$^{\bullet-}$ approaches that of HAn-6ANI-Ph-^{3}*NI, and so both RP and triplet are observed. Disappearance of the triplet spectrum indicates that the energy levels of MeOAn$^{\bullet+}$-6ANI-Ph-NI$^{\bullet-}$ at 250 K and of HAn$^{\bullet+}$-6ANI-Ph-NI$^{\bullet-}$ at 270 K lie slightly below their corresponding triplet states derived from CR, reducing $^3k_{ET}$, as reflected by the appearance, at later times, of a weak (a,e) RP signal via a triplet precursor. The energy level of Me$_2$NAn$^{\bullet+}$-6ANI-Ph-NI$^{\bullet-}$ lies below the energy level of Me$_2$NAn-6ANI-Ph-^{3}*NI even at 170 K, evidence that this triplet state is generated by CR of the primary RP Me$_2$NAn$^{\bullet+}$-6ANI$^{\bullet-}$-Ph-NI. At 270 K, no triplet spectra are expected for all three compounds.

Conclusions

In this study, we have demonstrated that TREPR spectroscopy of spin-polarized triplet states reveals the details of intramolecular electron-transfer dynamics within XAn-6ANI-Ph-NI donor−acceptor molecules having highly restricted conformations. Moreover, the importance of the microenvironment to both the energetics and dynamics of electron-transfer reactions in these molecules was demonstrated by using LC solvents. The substantial effect of temperature on the RPs energetics was demonstrated for all three triads. Thus, this methodology provides deeper insights into the different CS routes and their genesis, particularly when S−T mixing followed by CR generates the spin-polarized triplet state analogous to that found in native photosynthetic reaction centers and in a few model systems.

The picture that is beginning to emerge from the increasingly rich set of data on the spin dynamics of covalently linked RPs that we have obtained is one in which very subtle changes in the energy levels and in the distance and orientation of the radical ions relative to one another, as well as in the nature of the bonds connecting them, lead to profound changes in electronic coupling between the RPs. These changes in coupling translate directly into changes in the rates of CR. It is our goal that a better understanding of these dynamics will lead to structures in which the lifetime of the stored charges can be significantly enhanced by controlling the electronic coupling leading to CR.

Acknowledgment. This work is in fulfillment of the requirements for a M.Sc. degree (S.S.) at the Hebrew University of Jerusalem. The Farkas Center is supported by the Bundenministerium Forschung and Technologie and the Minerva Geselschaft für die Forschung GmbH. This work was partially supported by the U.S.-Israel BSF (H.L.). Discussions with Ulrich Heinen (University of Freiburg, Germany) are highly appreciated. We also thank the Ministry of Science, Culture and Sport for their financial support. Work at Northwestern University was supported by the Division of Chemical Sciences, Office of Basic Energy Sciences, U.S. Department of Energy (Grant No. DE-FG02-99ER14999) (M.R.W.).

JA034356X